

ADVANCED OPTICAL TECHNIQUES TO EXPLORE BRAIN STRUCTURE AND FUNCTION

L. SILVESTRI^{*,¶}, A. L. ALLEGRA MASCARO^{*}, J. LOTTI^{*},
L. SACCONI^{*,†} and F. S. PAVONE^{*,†,‡,§}

**European Laboratory for Nonlinear Spectroscopy (LENS)
University of Florence, Italy*

†National Institute of Optics (INO-CNR), Sesto Fiorentino, Italy

‡Department of Physics, University of Florence, Italy

*§International Center for Computational
Neurophotonics — ICON Foundation, Florence, Italy*

¶silvestri@lens.unifi.it

Accepted 17 October 2012

Published 31 January 2013

Understanding brain structure and function, and the complex relationships between them, is one of the grand challenges of contemporary sciences. Thanks to their flexibility, optical techniques could be the key to explore this complex network. In this manuscript, we briefly review recent advancements in optical methods applied to three main issues: anatomy, plasticity and functionality. We describe novel implementations of light-sheet microscopy to resolve neuronal anatomy in whole fixed brains with cellular resolution. Moving to living samples, we show how real-time dynamics of brain rewiring can be visualized through two-photon microscopy with the spatial resolution of single synaptic contacts. The plasticity of the injured brain can also be dissected through cutting-edge optical methods that specifically ablate single neuronal processes. Finally, we report how nonlinear microscopy in combination with novel voltage sensitive dyes allow optical registrations of action potential across a population of neurons opening promising prospective in understanding brain functionality. The knowledge acquired from these complementary optical methods may provide a deeper comprehension of the brain and of its unique features.

Keywords: Brain; optical microscopy; light sheet microscopy; two-photon microscopy.

1. Introduction

The brain is probably the most complex structure in the known universe, complex enough to coordinate movements, gather and organize lots of sensory

data, perform abstract reasoning and develop new ideas. Understanding the mechanisms underlying brain function is therefore one of the biggest challenges of contemporary science, considering also the increasing social impact of neurological disorders,

which are a primary cause of disability for millions of people worldwide.¹

Our current picture of the brain is that of an extremely complex circuit in which elementary computational units (neurons) exchange information between other units in the network through unidirectional links (synapses). The exceptional features of the brain appear to emerge from the enormous number of units and links and from the ability of the network to adaptively “rewire” itself in response to external and internal stimuli.² The investigation of the structural and dynamical properties of this network poses several challenges in imaging technology, since brain activity spans many orders of magnitude both spatially (from nanometers to centimeters) and temporally (from milliseconds to months). Thanks to their flexibility in terms of spatial and temporal resolution, together with high specificity, optical methodologies have recently become very popular in neuroscience research.³ In this paper, we will review specific optical microscopy strategies used to address three main questions in neuroscience, i.e., the micron-scale anatomy of entire brains, the structural plasticity *in vivo* and the functional connectivity of intact neuronal networks.

2. Whole-Brain High-Resolution Neuroanatomy

Although gross anatomical atlases of the brain are available, together with the detailed description of many types of neurons in terms of shape, functionality and genetic expression, we lack a complete map of neuronal connections on brain-wide scale. Such a map, which has been called “connectome”,⁴ is still out of reach because of the peculiar structure of the brain itself. In fact, although neuronal processes are very small in diameter (~ 100 nm), they typically extend over large distances, even throughout the whole brain.⁵ The pursuit of the connectome therefore needs imaging techniques capable of nanometric resolution (to distinguish adjacent processes) in centimeter-wide samples (to follow long-projecting axons across mouse brain). Electron microscopy (EM), the most popular technique with nanometric resolution, is however characterized by very slow data acquisition rates.⁶ In addition to imaging-related problems, whole brain studies with this method pose great challenges on the side of data management and analysis too. In

fact, mapping the relatively small brain of a mouse (1 cm^3) with such resolution will produce datasets exceeding the tens of PetaByte. As current information technology is not ready to cope with such datasets, technological efforts to achieve full-resolution connectomes risk to be useless at the moment. Although EM may be inappropriate for brain-wide studies, it has been successfully applied to reconstruct local circuitry in small regions,^{6,7} or the whole nervous system in very small organisms.⁸

The opposite of EM in terms of resolution is diffusion tensor imaging (DTI), a technique based on nuclear magnetic resonance. In this approach, the diffusion tensor of water molecules in the brain is used to infer the presence and local orientation of axonal fiber bundles.⁹ From the knowledge of the local orientation of fibers, it is possible to trace axonal bundles through the whole brain using a computational approach named tractography.¹⁰ Resolution in DTI is determined by the gradient of the static magnetic field and by the signal-to-noise ratio (S/N), which is ultimately limited by the acquisition time¹¹; typical resolution is never beyond some hundredths of micrometers.⁹ One of the main limitations of this method is the unspecificity of the contrast source, which gave rise to a large debate about the reliability and the interpretation of data produced by DTI.¹² Diffusion imaging remains, nevertheless, an extremely useful tool in neuroanatomy, since it is the only one which can be performed in living humans.

Light microscopy, which typically operates on the micron-scale, can bridge the gap between high resolution in small volumes and low resolution in the whole brain. In practice, however, it is impossible to reconstruct the full neuronal network with light microscopy, since its spatial resolution is limited by diffraction to ~ 200 nm, higher than the typical distance between processes. Nevertheless, using a sparse labeling approach, it is possible in principle to reconstruct selected neuronal systems throughout the whole brain with micron-scale resolution. Such meso-scale connectome or “projectome”, mapping long-range projections of small clusters of neurons,^{13,14} would in any case be extremely useful as little or none is known about the trajectories of brain-wide projections or about their variability between different individuals. However, in practice, no projection map has been produced hitherto. This is due to a combination of various factors. First of all, confocal or two-photon fluorescence (TPF)

microscopy, which are probably the most popular optical fluorescence techniques suited for volume imaging, are point-scanning techniques, with pixel dwell times of the order of milliseconds.¹⁵ Image acquisition rate is therefore still too low to cope with large volumes. Further, both confocal and TPF microscopy require the use of high-NA objective lenses,^{16,17} with limited working distances. The brain must then be cut into thin slices (no thicker than $\sim 50\ \mu\text{m}$ for confocal and $\sim 700\text{--}800\ \mu\text{m}$ for TPF imaging) which have to be matched after imaging. Surface distortion is more severe than in EM, since the tissue is not embedded in a hard resin and volume reconstruction is thus more challenging. Thanks to their high resolution and contrast, these methods are however very well suited for neuroanatomical studies regarding brain subregions¹⁸ or small animals.¹⁹ On the other hand, optical imaging of entire resin-embedded mouse brains, coupled to automatic tissue slicing, has been recently proposed.^{20,21} This approach, however, relies on a Golgi-based staining which, unlike fluorescence labeling, is nonspecific, thereby restricting its applicability.

The inherent limitations of confocal and TPF microscopy have been overcome by light-sheet microscopy (LSM), which allows fast fluorescence imaging with high resolution in large specimens.²² Although light-sheet illumination was introduced in microscopy more than a century ago,²³ it has been applied to fluorescence imaging of biological specimens only in recent years. After the seminal paper of Voie *et al.* in 1993,²⁴ LSM has known a true renaissance, thanks to its characteristic advantages: intrinsic optical sectioning, high frame rate, high S/N, low phototoxicity and photobleaching.^{22,25–31}

In LSM, the sample is illuminated with a thin sheet of light, and the fluorescence emission is collected along the axis perpendicular to the illumination plane³² (see Fig. 1). As the illumination and detection path are decoupled, optical sectioning can be achieved in LSM in wide-field detection architecture, guaranteeing fast imaging over a large field of view. When applied to large specimens, LSM is often coupled with a procedure to clear tissues based on refractive index matching²⁴ (see Fig. 2). Index-matching liquids used to effectively clear tissue for LSM, such as Benzyl Alcohol/Benzyl Benzoate (BABB), are immiscible with water, restricting their use to fixed tissue and in combination with a dehydration procedure.³³ Due to their low biocompatibility, even other clearing methods that relies on

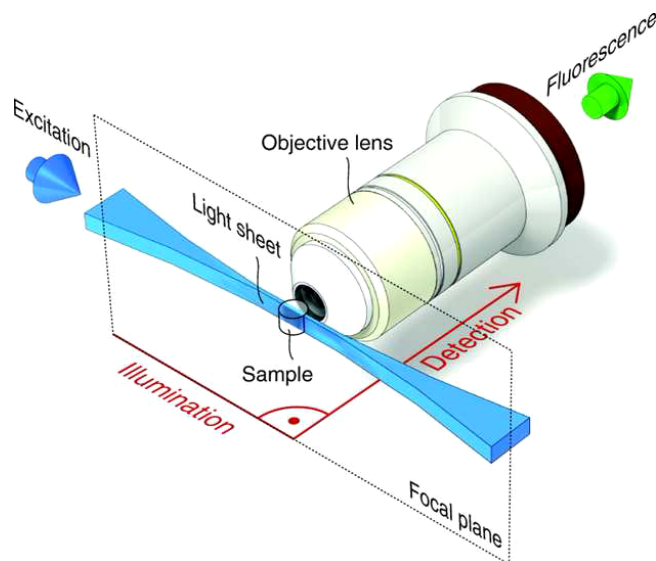


Fig. 1. Simplified scheme of a light sheet illumination microscope. The light sheet lies in the focal plane of the detection objective. Fluorescence and excitation light are indicated in green and blue, respectively. Reproduced with permission from Ref. 32.

water soluble agents, such as glycerol,³⁴ are generally not suitable for *in vivo* investigations.

Dotz *et al.* pioneered the application of LSM coupled with optical clearing to image GFP-labeled mouse brains.²⁵ With this approach, they were able to reconstruct the neuronal network of pyramidal neurons inside excised hippocampus with sub-cellular resolution. Although this method allowed sub-cellular high-contrast imaging in excised regions, sample-induced light scattering prevents high-resolution imaging in the whole brain. In fact, the residual sample-induced scattering that still affects a cleared brain expands the excitation light sheet (leading to out-of-focus contributions) and blurs the collected fluorescence images. To recover the partially lost optical sectioning and image contrast, structured illumination approaches have been combined with LSM. Patterned illumination can be provided by either using a grid in a conjugated optical plane^{35–37} or by an AOM coupled with a galvo mirror.³⁸ All these approaches share several drawbacks. In fact, many images have to be collected to synthesize the final one, reducing the effective frame rate attainable. Furthermore, out-of-focus filtering is performed only after detection; the effective dynamic range of the detector is thus strongly reduced since a lot of background photons are uselessly collected.³⁹

To exploit the detector's full dynamic range, line confocal detection coupled with scanning illumination

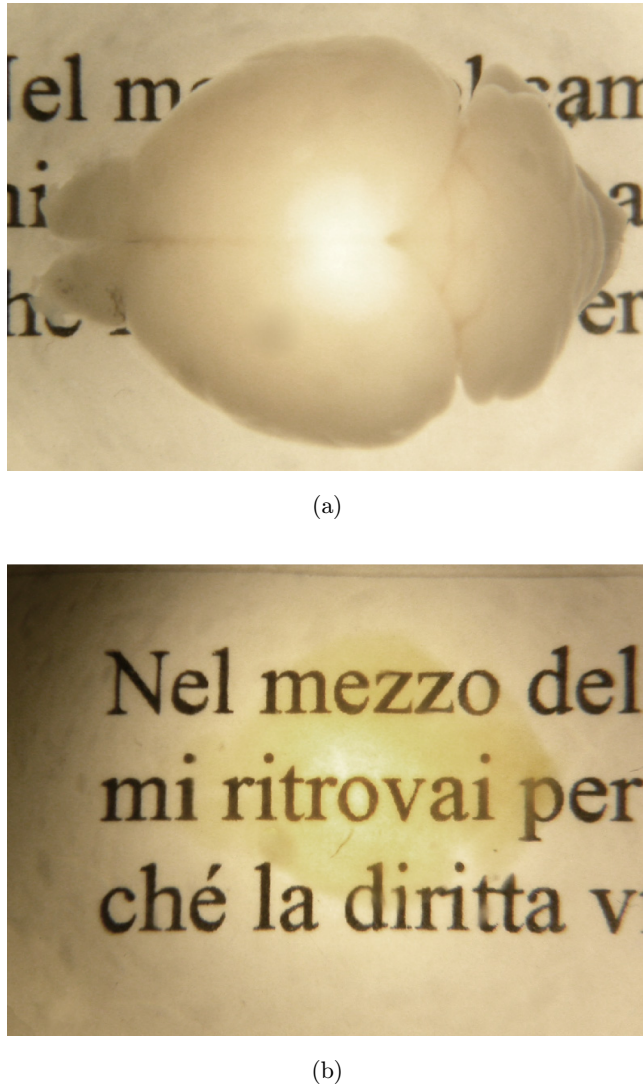


Fig. 2. Optical clearing through refractive index matching. A mouse brain before (a) and after (b) optical clearing by substitution of water with a mixture 1:2 of Benzyl Alcohol and Benzyl Benzoate.

has been proposed.^{40,41} In the scheme described by Fahrbach and Rohrbach, confocal detection is achieved by exposing the camera at each position of the excitation line and subsequently retaining only the pixel line confocal to the excitation beam.⁴⁰ Although this confocal approach allows a significant enhancement of image contrast, the camera needs to be exposed and readout at each beam position to produce a single final image of the whole field of view, and background rejection is achieved by post-processing the acquired data.

We recently described an optical method, confocal light sheet microscopy (CLSM), in which the out-of-focus background rejection based on confocal

detection is achieved in real time.⁴¹ CLSM synergically combines the advantages of LSM, in terms of fast acquisition time and low photobleaching rate, with the spatial filtering capability of a confocal approach. The key feature of CLSM is a spatial filter that selects only ballistic fluorescence photons emitted from the focal plane of detection optics, i.e., from fluorophores excited by ballistic illumination photons (see Fig. 3). The real-time contrast enhancement of CLSM (see Fig. 4) allows reconstructing a

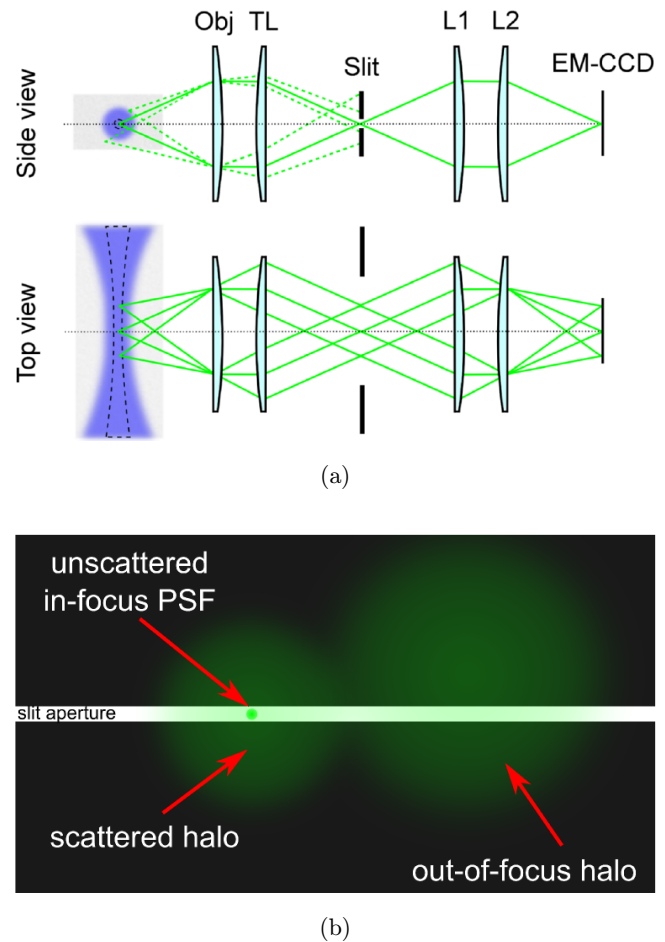


Fig. 3. CLSM operating principle. In (a) side (upper panel) and top (lower panel) views of the spatial filter operation scheme. The diffraction limited excitation beam (black dashed line) is blurred (blue area) because of sample-induced scattering. The fluorescence light is then emitted both in-focus (green continuous lines) and out-of-focus (green dashed lines): only the in-focus ballistic photons are properly focused in the aperture of the spatial filter (Slit) by the first 4f optical system (objective, Obj and tube lens, TL). The second 4f system (L1, L2) images ballistic photons on the EM-CCD sensor. In (b) view of the slit plane [black line in (a)]. In-focus unscattered fluorescence emission is correctly focused into the slit, whilst both scattered and out-of-focus light forms a wide halo which lies almost completely outside the aperture and is therefore blocked.

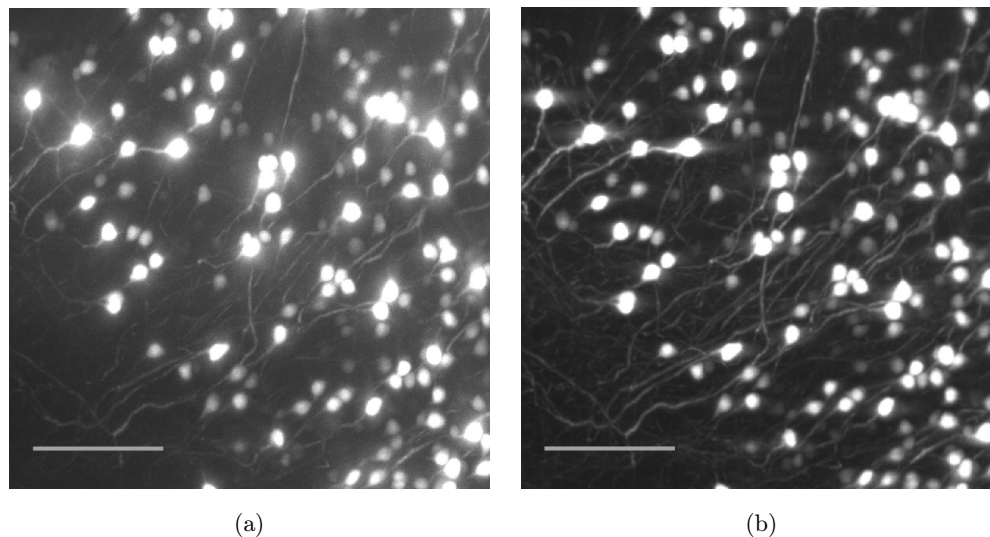


Fig. 4. Contrast enhancement in CLSM. Conventional LSM (a) and corresponding CLSM image (b) of a portion of hippocampus of a thy1-GFP-M mouse (post-natal day 23, PND 23). The EMCCD was overexposed, saturating cell bodies, to better distinguish neurites. Images are maximum intensity projections of 600 sections (z -step $1\ \mu\text{m}$).

fluorescently labeled entire mouse brain, with microscopic three-dimensional resolution.

Although this method provides high-resolution 3D reconstruction of the entire brain anatomy, CLSM offers just a single snapshot of the action. In fact, the brain is constantly reshaping its structure in terms of axonal remodeling and synaptic plasticity in response to external stimuli. This dynamical remodeling needs to be investigated *in vivo*.

3. *In Vivo* Structural Plasticity of the Brain

The term “structural plasticity” refers to all the changes in the anatomical connectivity between neurons through modifications of synaptic connectivity patterns, variation in synapse number, re-routing of axonal and dendritic branching patterns and, last, alteration in neuronal cell numbers. Structural plasticity plays a major role during development, when continuously new connections are established and refined.^{42–46} Still when development is complete, structural modifications such as the dynamic formation, modification and pruning of dendritic spines⁴⁷ and the re-routing of axonal branches within cortical columns^{48,49} spontaneously occur.

High resolution *in vivo* optical imaging of the brain poses several challenges. In fact, as described in Sec. 2, clearing methodologies cannot be employed

in living animals, limiting the penetration depth affordable with conventional linear optical techniques. A possible solution to increase the penetration depth is based on the photo-acoustic effect,⁵⁰ allowing deeper imaging inside living tissue, up to several millimeters. Exploiting its high penetration depth, photo-acoustic microscopy (PAM) has been recently used to image the whole vascular network of living mice.⁵¹ PAM enables deeply penetrating functional and molecular imaging at high spatial resolution but, since it does not directly rely on fluorescence labeling, until now this technique has not had the same fundamental impact on biomedical research of existing high-resolution optical imaging methodologies such as TPF microscopy.¹⁷

In fact, allowing high-resolution fluorescence imaging in scattering samples, TPF microscopy has totally revolutionized the research in neuroplasticity in the last years.^{52,53} The first application of TPF to neurobiology exploited its exquisite resolution in scattering tissue to image the structure and function of dendritic spines in brain slices. Recently, time-lapse TPF microscopy has been employed to directly monitor the dynamics of synaptic structures in the intact murine neocortex.

Several groups, employing different transgenic models, focused their attention on either the pre-synaptic (i.e., axonal bouton or varicosity) or the post-synaptic (i.e., dendritic spine) portion of the inter-neuronal contact. For example, time-lapse

TPF imaging of dendritic structural plasticity provided support for a direct correlation between spine turnover and experience-dependent plasticity⁵⁴ (see Fig. 5). Increased spine and synapse densities have been previously reported after training in enriched

environments,^{55–60} as well as after long-term sensory stimulation⁶¹ and deprivation.⁴⁶ These studies reveal that spine addition and subtraction are likely to contribute to experience-dependent rewiring of cortical circuits.

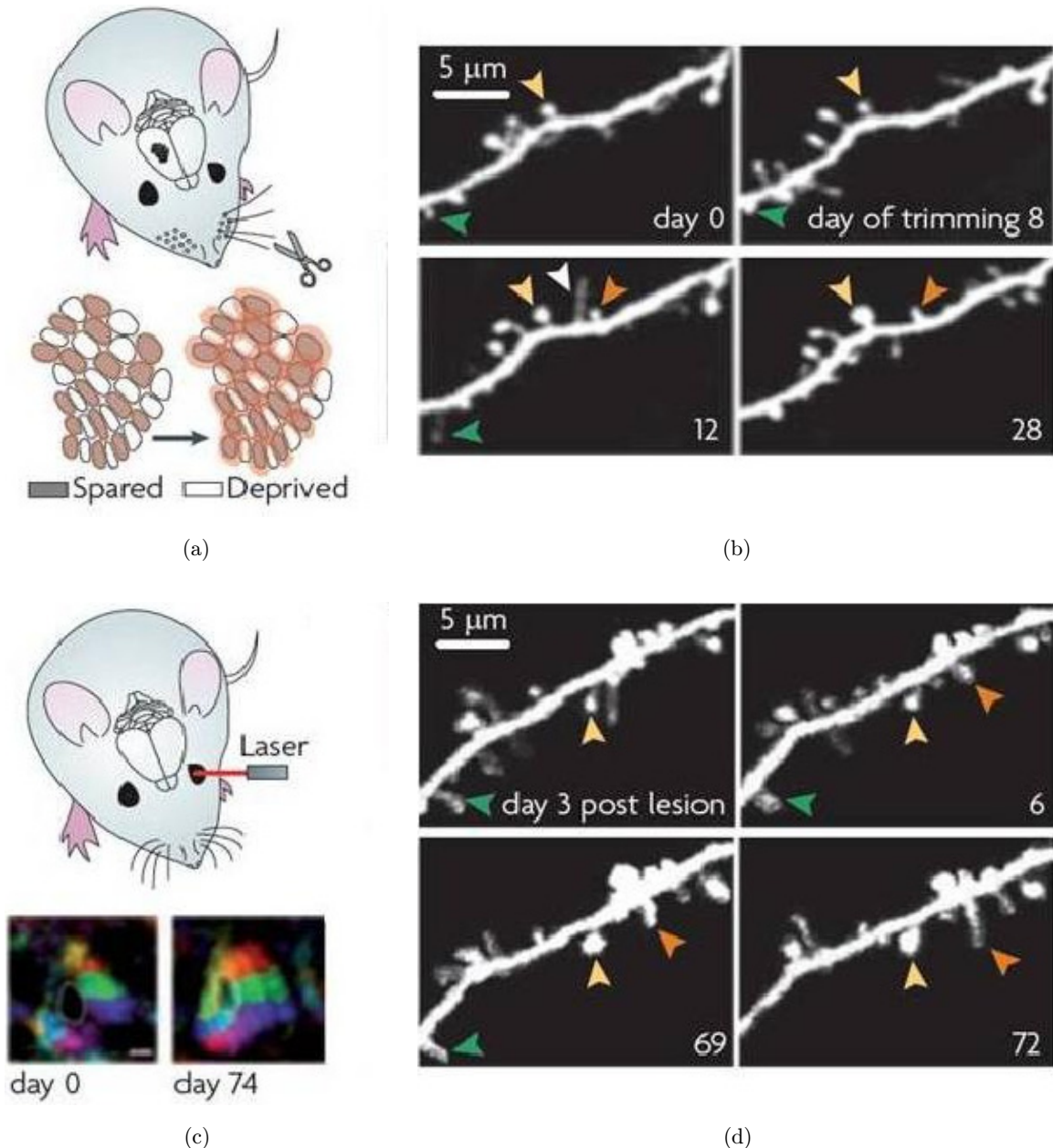


Fig. 5. Experience-dependent spine plasticity in the adult neocortex. (a) Chessboard whisker trimming causes changes in the whisker representational map in the barrel cortex. (b) Time-lapse TPF images of dendritic spines in the barrel cortex before and after chessboard whisker trimming. Many spines are stable (yellow arrowhead), but some appear and disappear (white arrowhead). New persistent spines (orange arrowhead) are more likely to grow after whisker trimming, whilst previously persistent spines (green arrowhead) are more likely to disappear. (c) Immediately after a focal lesion in the retina the lesion projection zone in the neocortex is unresponsive to visual stimulation, as measured by intrinsic signal optical imaging (bottom, day 0). The size of the unresponsive region decreases with time. Scale bar, 700 μm . (d) Time-lapse of dendritic spines in the visual cortex after unilateral focal lesion in the retina. Although some spines are present over more than two months of imaging (yellow arrowhead), most spines are lost (green arrowhead) and replaced by new persistent spines (orange arrowhead). Adapted with permission from Ref. 112.

In addition, morphological rearrangements of neurons and glial cells may be involved in recovery from neuronal injury.^{62–64} Despite long-held dictum stating the incapability of adult brain and spinal cord to regenerate after injury, reactive structural plasticity may occur in particular conditions and possibly play a role in recovery from brain trauma.^{62,65} Technical issues so far limited the investigation of the biological mechanisms of the reactive plasticity after injury in the adult central nervous system (CNS). The main obstacle to a full comprehension concerns the targeted manipulation of CNS neurons. In fact, conventional injury models (e.g., pharmacological approaches) produce massive degeneration and lack the specificity required to univocally identify the promoter of the injury-induced reactive plasticity.⁶⁶ Besides imaging, the spatial localization of multi-photon absorption¹⁷ can indeed be exploited to perform *in vivo* selective lesions on single cellular compartments without causing any visible collateral damage to the surrounding neuronal structures. The first published report of femtosecond laser sub-cellular nanosurgery was by Koenig *et al.*,⁶⁷ who demonstrated the potential of this technique by ablating nanometer-sized regions of the genome within the nucleus of living cells. Following this seminal work, laser nanosurgery has been applied in living cells to investigate the biological function of sub-cellular compartments, like mitochondria or microtubules.^{68–71} A similar approach has also been applied in living animals, where two-photon imaging and laser-induced lesions have been combined. For example, femtosecond laser ablations allowed the characterization of the complex events associated with embryo development

in vivo.⁷² Laser nanosurgery has been demonstrated in the mammalian CNS as well.^{73,74} The high spatial precision of multi-photon laser nanosurgery allows ablating even individual dendritic spines, while sparing the adjacent spines and the structural integrity of the dendrite (see Fig. 6). Furthermore, laser-induced lesions have been used to damage the blood–brain barrier⁷⁵ and to produce targeted highly confined stroke.⁷⁶

TPF microscopy is an optimal tool not only to detect structural rearrangements in time but also to monitor functional changes at the cellular level. Fluorescent ion-selective probes, which allow real-time imaging of cellular movements of physiologically relevant ions, are well suited for this purpose. Between the different types of indicators developed, the most commonly used detect concentration changes of the $[Ca^{2+}]$ ion. Imaging methods can probe $[Ca^{2+}]$ dynamics with sub-micrometer spatial and sub-millisecond temporal resolutions.⁷⁷ The sensitivity of two-photon imaging of calcium dynamics allowed the detection of a single $[Ca^{2+}]$ -permeable channel opening.^{78–80} Similar measurements have been used to analyze $[Ca^{2+}]$ variations in dendrites^{81–84} and pre-synaptic boutons.^{85–87}

Unfortunately, fluorescence changes through $[Ca^{2+}]$ indicators are not straightforwardly related to the number of action potentials or spike timing. It is sometimes possible to detect sawtooth-shaped fluorescence transients corresponding to single spikes,^{88–91} but the numerous noise sources in the intact preparation may prevent single action potential detection. On the other hand, membrane potential can be directly probed by specific voltage sensitive dyes (VSDs).

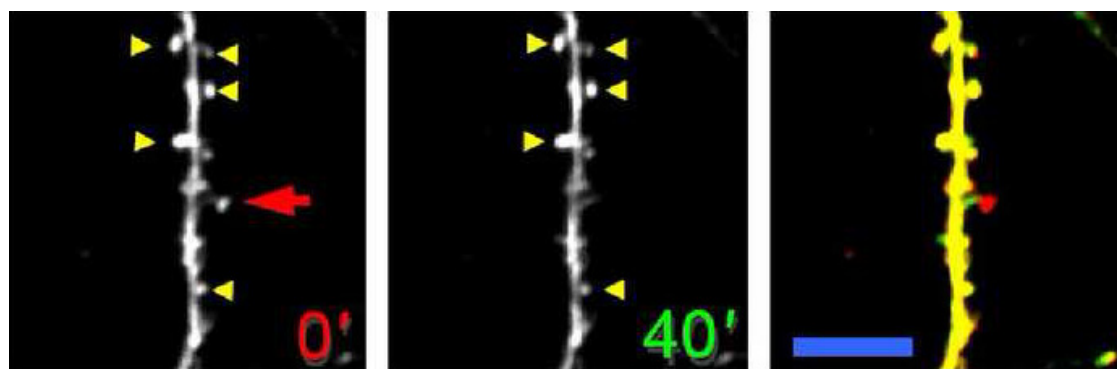


Fig. 6. Laser ablation of a single dendritic spine. Images of a portion of a dendrite before and 40 min after spine ablation. The yellow arrowheads indicate some stable spines on the irradiated dendrite. Scale bar, 15 μm . Modified from Ref. 73.

4. Optical Recording of Action Potentials

The most popular method to record electrical activity in neurons is the patch-clamp, introduced by Neher and Sakmann in 1976.⁹² Although this technique allows precise voltage measurements in single cells, it can be hardly applied to many neurons at once, given the steric hindrance of the electrodes. Parallel large-area electric measurements are possible using micro-electrode arrays,^{93,94} which however measure an average electric field rather than the membrane potential of single neurons. Furthermore, the position of the electrodes is imposed by the geometry of the array itself.

Current optical techniques for recording membrane potential can overcome these issues. The use of light to detect electrical field variations across the cell membrane was pioneered in the 1970s by Lawrence Cohen,⁹⁵ who devised the first VSD, i.e., dyes in which change in the membrane potential alters some optically observable parameter (e.g., fluorescence).⁹⁶ VSDs are commonly used in combination with linear microscopy techniques, limiting their application to *in vitro* samples or to the most superficial layers of biological tissues. In fact, the light scattering that occurs into the tissue dramatically degrades the resolution and/or S/N of the acquired images. As described in the previous section, nonlinear microscopy guarantees micron-scale resolution in deep scattering tissues. The main nonlinear techniques used in combination with VSDs are TPF and second-harmonic generation (SHG).^{17,97,98} The former is an incoherent process in which two photons are absorbed almost simultaneously by the molecule to reach an excited state, and a single photon is spontaneously emitted after a variable amount of time (of the order of ns). On the other hand, SHG is a coherent phenomenon where two low-energy photons are transformed in a single high-energy one, without absorption. Due to the coherence requirement, SHG signal is much stronger when harmonophores (molecules operating the frequency doubling) are positioned in an ordered rather than random fashion. SHG thus gives a more contrasted image of cell membranes than TPF.^{99,100} For this reason, SHG imaging of VSDs has been recently exploited to optically detect action potentials in model membranes,¹⁰¹ in cultured neurons of *Aplysia*^{102,103} and in mammalian intact neuronal systems.^{104,105} In these examples, the optical

recording of neuronal APs was performed only in a single position of the neuron using a line scanning procedure. In principle, action potentials in several neurons can be recorded at a sampling frequency of more than 1 kHz by scanning the beam in multiple selected lines. This cannot be achieved with a standard galvo mirror since the time required to reach and stabilize a new position is about 1 ms. Scanning a set of points within a plane at high speed is possible using acousto-optic deflectors (AODs). In an AOD, a propagating ultrasonic wave establishes a grating that diffracts a laser beam at a precise angle which can be changed within a few microseconds.

The first implementation of a high-speed, random-access, laser-scanning fluorescence microscope configured to record fast physiological signals from small neuronal structures with high spatiotemporal resolution has been presented by Bullen *et al.*¹⁰⁶ Recently, the advantages of SHG were combined with a random access excitation scheme¹⁰⁷ to develop a new microscope (random-access second-harmonic, RASH) capable of recording neuronal electrical activity in living tissue, in several cells simultaneously, with a high spatial (sub-cellular) and temporal (sub-millisecond) resolution. The RASH microscope, in combination with a SHG VSD (FM4-64), was used to simultaneously record evoked electrical activity from clusters of Purkinje cells in acute cerebellar slices. Complex spikes, both synchronous and asynchronous, were optically recorded simultaneously across a given population of neurons averaging 20 trials (see Fig. 7). Spontaneous electrical activity was also monitored simultaneously in pairs of neurons, where action potentials were recorded in single sweep (without averaging across trials).

In order to apply this methodology in live animals, an epi-fluorescence collection is needed. Unfortunately, only a small fraction of the SHG signal can be epi-collected. Therefore, to explore the possibility of optical recording action potential in multiple neurons simultaneously *in vivo*, we tested the efficiency and sensitivity of a promising TPF VSD, di-3-ANEPPDHQ,¹⁰⁸ in random access modality. The microscope was modified to epi-collect TPF signal¹⁰⁹ (see Fig. 8); the sensitivity and S/N of this dye was investigated in TPF by using an excitation wavelength of 1064 nm and a 655/40 nm band-pass emission filter. In experimental configuration, spontaneous electrical activity was monitored

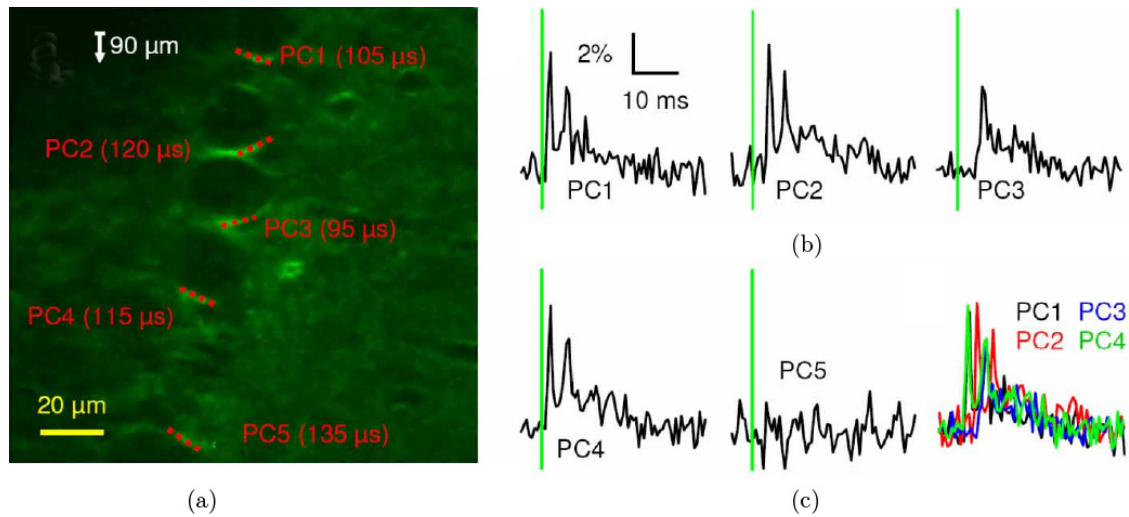


Fig. 7. Optical multi-unit recording of stimulated electrical activity. (a) SHG image of a cerebellar slice taken at a depth of $90 \mu\text{m}$. The multi-unit SHG recording was carried out from the lines drawn (dotted red) on the 5 Purkinje cells (PCs), with the integration time per membrane pass indicated. (b) Multiplexed recording of action potentials from the 5 PCs following stimulation of climbing fibers (green lines). The relative SHG variation ($\Delta\text{SHG}/\text{SHG}$) is shown as a function of time. Each trace represents the average of 20 trials for each PCs. The time resolution is 0.47 ms. (c) Superposition of SHG traces corrected for multiplex delay is shown. PC5 is not shown since it was quiescent. From Ref. 107.

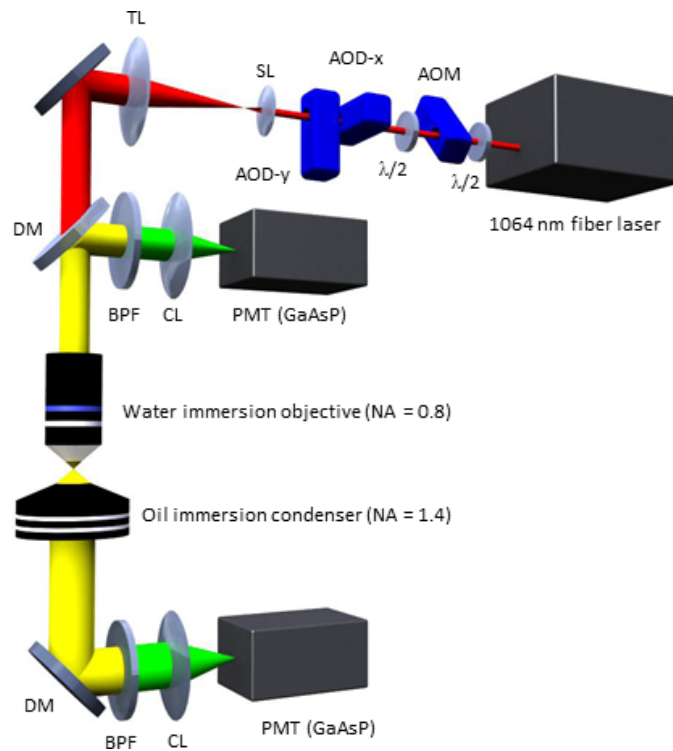


Fig. 8. Random access multi-photon (RAMP) microscope. A fiber laser provides the excitation light, which comprises 200 fs width pulses at 80 MHz repetition rate. The laser beam is adjusted for optimal linear polarization via a half-wave ($\lambda/2$) plate. Beam passes are made through 45° AOM for angular spreading pre-compensation. A second half-wave ($\lambda/2$) plate is placed after the AOM to optimize the diffraction efficiencies of the two orthogonally mounted AODs (AOD- x and AOD- y). A scanning lens (SL) and a microscope tube lens (TL) expand the beam before it is focused onto the specimen by the objective lens. The TPF signal is trans- and epi-collected by an oil immersion condenser and the excitation objective, respectively. Dichroic mirrors (DM) separates excitation and fluorescence light. This latter is then band-pass filtered (BPF) and focused by two collection lenses (CL) into two GaAsP PMTs.

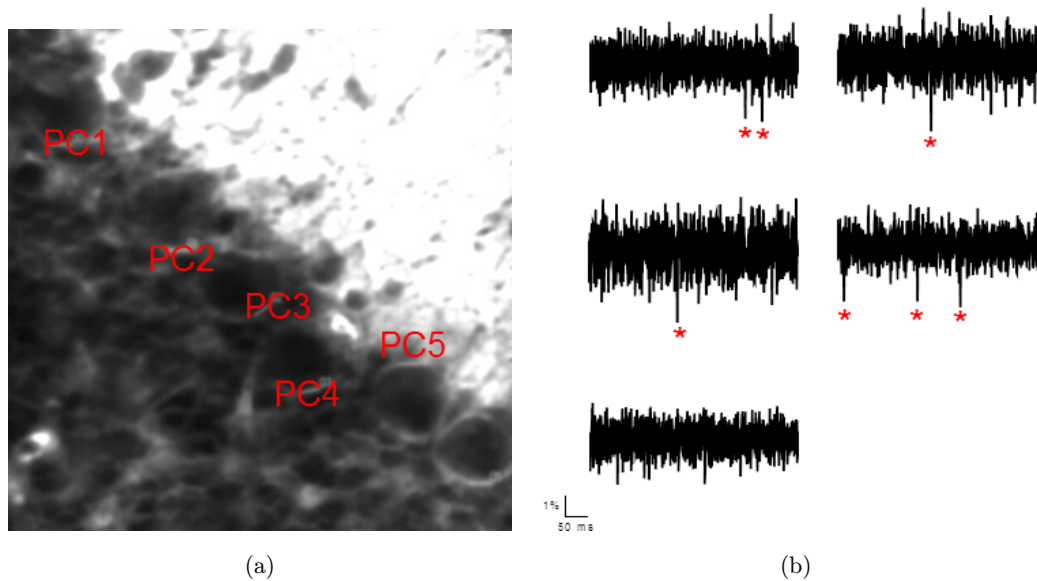


Fig. 9. Optical multi-unit recording of spontaneous electrical activity. (a) TPF image of a cerebellar slice taken at a depth of $90\ \mu\text{m}$. The multi-unit TPF recording was carried out on 5 PCs, with membrane integration time per neuron $\approx 90\ \mu\text{s}$. (b) Multiplexed recording of spontaneous electrical activity from the 5 PCs. The relative fluorescence variation ($\Delta F/F$) is shown as a function of time. Single action potentials are clearly visible and are indicated by red stars.

in five neurons simultaneously with a S/N value that is sufficient to detect single action potential above the shot noise (see Fig. 9).

These results show the strength of this technique in describing the temporal dynamics of neuronal assemblies opening promising prospective in understanding the computations of neuronal networks.

5. Conclusion

The brain is one of the most poorly understood organs of our body. Its dynamics spans several orders of magnitude both spatially and temporally, challenging current imaging technologies. Taking advantage of their intrinsic flexibility, optical

techniques have been applied to study several issues in neuroscience. Here we focused on three specific applications, showing how light microscopy can be used to study fine anatomy, plasticity and neuronal functionality. In Table 1, we summarized the main features of the different techniques described throughout the paper.

The high resolution, contrast and frame rate affordable, thanks to the last improvements in fluorescence LSM, will allow the investigation, at the cellular level, of specific neuronal systems throughout the whole brain. For instance, projection of localized nuclei (like monoaminergic systems), thalamo-cortical circuitry, inter-hemispheric connections can be traced, opening promising

Table 1. Comparison of different techniques for structural and functional brain imaging.

Technique	Spatial resolution	Temporal resolution	<i>In vivo</i>	Contrast source
EM	$\sim 15 \times 15 \times 50\ \text{nm}^3$	$< 10\ \mu\text{m}^3/\text{s}$	–	Electron absorption or scattering
CM	$\sim 0.25 \times 0.25 \times 0.5\ \mu\text{m}^3$	$\sim 10^4\ \mu\text{m}^3/\text{s}$	+	Fluorescence
TPM	$\sim 0.5 \times 0.5 \times 1\ \mu\text{m}^3$	$\sim 10^4\ \mu\text{m}^3/\text{s}$	+	Fluorescence
LSM	$\sim 2 \times 2 \times 9\ \mu\text{m}^3$	$\sim 10^6\ \mu\text{m}^3/\text{s}$	–	Fluorescence
PAM	$\sim 45 \times 45 \times 15\ \mu\text{m}^3$	$\sim 10^7\ \mu\text{m}^3/\text{s}$	+	Light absorption
MRI	$> 150 \times 150 \times 300\ \mu\text{m}^3$	$\sim 10^9\ \mu\text{m}^3/\text{s}$	+	Nuclear magnetic resonance of hydrogen nuclei

Electron microscopy (EM), confocal microscopy (CM), two-photon microscopy (TPM), light sheet microscopy (LSM), photo-acoustic microscopy (PAM) and magnetic resonance imaging (MRI) are compared, highlighting their spatial and temporal resolution, *in vivo* applicability and contrast source.

prospective for understanding the large-scale brain connectivity.

The dynamic remodeling of the brain connectivity can be explored *in vivo* by nonlinear optical techniques. Two-photon microscopy has revolutionized high-resolution imaging of neuronal plasticity since it is endowed with the extraordinary capability of providing access into the intact brain *in vivo*. In combination with genetic manipulation tools to introduce, modify, or dismiss characters from the biological scene, two-photon microscopy opens the way to unhinge the neurobiological mechanisms underlying remodeling events, shedding light on the various mechanisms of neuronal plasticity by which the brain continuously rewires itself.

The combination of nonlinear microscopy with innovative ultrafast scanning modalities, allows simultaneous detection of spontaneous electrical activity of several neurons in single trial recording. Random accesses microscopy can be potentially combined with laser stimulation methods, e.g., uncaging of neurotransmitters¹¹⁰ or opsin-based genetic tools,¹¹¹ to define the connectivity of neuronal circuits in an unprecedented interactive manner.

Integration of various imaging techniques, as the ones described in this review, could eventually allow mining the complex interaction between structure and function which give rise to the unique capabilities of the brain.

Acknowledgments

The research leading to these results has received funding from the European Union Seventh Framework Programme (FP7/2007-2013) under Grant agreements Nos. 228334 and 241526. This research project has also been supported by Human Frontier Science Program research grant (RGP0027/2009) and by the Italian Ministry for Education, University and Research in the framework of the Flagship Project Nanomax and by Italian Ministry of Health in the framework of the “Stem cells call for proposals”. This research has been carried out in the framework of the research activities of ICON foundation supported by “Ente Cassa di Risparmio di Firenze”.

References

1. J. A. Aarli, T. D. Uca, A. Janca, A. Muscetta, “Neurological disorders: Public health challenges,” World Health Organization ISBN 9241563362 (2006).

2. D. V. Buonomano, M. M. Merzenich, “Cortical plasticity: From synapses to maps,” *Ann. Rev. Neurosci.* **21**, 149–186 (1998).
3. B. A. Wilt *et al.*, “Advances in light microscopy for neuroscience,” *Ann. Rev. Neurosci.* **32**, 435–506 (2009).
4. O. Sporns, G. Tononi, R. Kotter, “The human connectome: A structural description of the human brain,” *PLoS Comput. Biol.* **1**, e42 (2005).
5. J. W. Lichtman, W. Denk, “The big and the small: Challenges of imaging the brain’s circuits,” *Science* **334**, 618–623 (2011).
6. M. Helmstaedter, K. L. Briggman, W. Denk, “High-accuracy neurite reconstruction for high-throughput neuroanatomy,” *Nat. Neurosci.* **14**, 1081–1088 (2011).
7. K. L. Briggman, M. Helmstaedter, W. Denk, “Wiring specificity in the direction-selectivity circuit of the retina,” *Nature* **471**, 183–188 (2011).
8. J. G. White, E. Southgate, J. N. Thomson, S. Brenner, “The structure of the nervous system of the nematode *Caenorhabditis elegans*,” *Philos. Trans. Roy. Soc. London B Biol. Sci.* **314**, 1–340 (1986).
9. S. Mori, J. Zhang, “Principles of diffusion tensor imaging and its applications to basic neuroscience research,” *Neuron* **51**, 527–539 (2006).
10. K. Yamada, K. Sakai, K. Akazawa, S. Yuen, T. Nishimura, “MR tractography: A review of its clinical applications,” *Magn. Reson. Med. Sci.* **8**, 165–174 (2009).
11. P. V. Prasad, *Magnetic Resonance Imaging: Methods and Biologic Applications*, Humana Press (2006).
12. A. L. Alexander, J. E. Lee, M. Lazar, A. S. Field, “Diffusion tensor imaging of the brain,” *Neurotherapeutics* **4**, 316–329 (2007).
13. J. W. Bohland *et al.*, “A proposal for a coordinated effort for the determination of brainwide neuroanatomical connectivity in model organisms at a mesoscopic scale,” *PLoS Comput. Biol.* **5**, e1000334 (2009).
14. N. Kasthuri, J. W. Lichtman, “The rise of the “projectome,”” *Nat. Methods* **4**, 307–308 (2007).
15. J. B. Pawley, *Handbook of Biological Confocal Microscopy*, Springer (2006).
16. R. H. Webb, “Confocal optical microscopy,” *Rep. Prog. Phys.* **59**, 427–471 (1996).
17. W. R. Zipfel, R. M. Williams, W. W. Webb, “Nonlinear magic: Multiphoton microscopy in the biosciences,” *Nat. Biotechnol.* **21**, 1369–1377 (2003).
18. H. Hama *et al.*, “Scale: A chemical approach for fluorescence imaging and reconstruction of transparent mouse brain,” *Nat. Neurosci.* **14**, 1481–1488 (2011).

19. T. L. Tay, O. Ronneberger, S. Ryu, R. Nitschke, W. Driever, "Comprehensive catecholaminergic projectome analysis reveals single-neuron integration of zebrafish ascending and descending dopaminergic systems," *Nat. Commun.* **2**, 171 (2011).
20. D. Mayerich, L. Abbott, B. McCormick, "Knife-edge scanning microscopy for imaging and reconstruction of three-dimensional anatomical structures of the mouse brain," *J. Microsc.* **231**, 134–143 (2008).
21. A. Mascaro, M. Farina, R. Gigli, C. E. Vitelli, L. Fortunato, "Recent advances in the surgical care of breast cancer patients," *World J. Surg. Oncol.* **8**, 5 (2010).
22. J. Huisken, J. Swoger, F. Del Bene, J. Wittbrodt, E. H. Stelzer, "Optical sectioning deep inside live embryos by selective plane illumination microscopy," *Science* **305**, 1007–1009 (2004).
23. H. Siedentopf, R. Zsigmondy, "Über sichtbarmachung und größenbestimmung ultramikroskopischer teilchen, mit besonderer anwendung auf gold-rubingläser," *Ann. Phys.* **315**, 1–39 (1902).
24. A. H. Voie, D. H. Burns, F. A. Spelman, "Orthogonal-plane fluorescence optical sectioning: Three-dimensional imaging of macroscopic biological specimens," *J. Microsc.* **170**, 229–236 (1993).
25. H. U. Dodt *et al.*, "Ultramicroscopy: Three-dimensional visualization of neuronal networks in the whole mouse brain," *Nat. Methods* **4**, 331–336 (2007).
26. J. Huisken, D. Y. Stainier, "Even fluorescence excitation by multidirectional selective plane illumination microscopy (mSPIM)," *Opt. Lett.* **32**, 2608–2610 (2007).
27. P. J. Verwee *et al.*, "High-resolution three-dimensional imaging of large specimens with light sheet-based microscopy," *Nat. Methods* **4**, 311–313 (2007).
28. P. J. Keller, A. D. Schmidt, J. Wittbrodt, E. H. Stelzer, "Reconstruction of zebrafish early embryonic development by scanned light sheet microscopy," *Science* **322**, 1065–1069 (2008).
29. C. Dunsby, "Optically sectioned imaging by oblique plane microscopy," *Opt. Express* **16**, 20,306–20,316 (2008).
30. T. F. Holekamp, D. Turaga, T. E. Holy, "Fast three-dimensional fluorescence imaging of activity in neural populations by objective-coupled planar illumination microscopy," *Neuron* **57**, 661–672 (2008).
31. M. Tokunaga, N. Imamoto, K. Sakata-Sogawa, "Highly inclined thin illumination enables clear single-molecule imaging in cells," *Nat. Methods* **5**, 159–161 (2008).
32. J. Huisken, D. Y. Stainier, "Selective plane illumination microscopy techniques in developmental biology," *Development* **136**, 1963–1975 (2009).
33. K. Becker, N. Jahrling, S. Saghafi, R. Weiler, H. U. Dodt, "Chemical clearing and dehydration of GFP expressing mouse brains," *PLoS One* **7**, e33916 (2012).
34. V. V. Tuchin, "Optical clearing of tissues and blood using the immersion method," *J. Phys. D Appl. Phys.* **38**, 2497–2518 (2005).
35. T. Breuninger, K. Greger, E. H. Stelzer, "Lateral modulation boosts image quality in single plane illumination fluorescence microscopy," *Opt. Lett.* **32**, 1938–1940 (2007).
36. S. Kalchmair, N. Jahrling, K. Becker, H. U. Dodt, "Image contrast enhancement in confocal ultramicroscopy," *Opt. Lett.* **35**, 79–81 (2010).
37. J. Mertz, J. Kim, "Scanning light-sheet microscopy in the whole mouse brain with HiLo background rejection," *J. Biomed. Opt.* **15**, 016027 (2010).
38. P. J. Keller *et al.*, "Fast, high-contrast imaging of animal development with scanned light sheet-based structured-illumination microscopy," *Nat. Methods* **7**, 637–642 (2010).
39. J. Mertz, "Optical sectioning microscopy with planar or structured illumination," *Nat. Methods* **8**, 811–819 (2011).
40. F. O. Fahrbach, A. Rohrbach, "Propagation stability of self-reconstructing Bessel beams enables contrast-enhanced imaging in thick media," *Nat. Commun.* **3**, 632 (2012).
41. L. Silvestri, A. Bria, L. Sacconi, G. Iannello, F. S. Pavone, "Confocal light sheet microscopy: Microscale neuroanatomy of the entire mouse brain," *Opt. Express* **20**, 20,582–20,598 (2012).
42. A. Antonini, M. P. Stryker, "Rapid remodeling of axonal arbors in the visual cortex," *Science* **260**, 1819–1821 (1993).
43. A. K. Majewska, J. R. Newton, M. Sur, "Remodeling of synaptic structure in sensory cortical areas *in vivo*," *J. Neurosci.* **26**, 3021–3029 (2006).
44. C. Portera-Cailliau, R. M. Weimer, V. De Paola, P. Caroni, K. Svoboda, "Diverse modes of axon elaboration in the developing neocortex," *PLoS Biol.* **3**, e272 (2005).
45. E. S. Ruthazer, C. J. Akerman, H. T. Cline, "Control of axon branch dynamics by correlated activity *in vivo*," *Science* **301**, 66–70 (2003).
46. Y. Zuo, G. Yang, E. Kwon, W. B. Gan, "Long-term sensory deprivation prevents dendritic spine loss in primary somatosensory cortex," *Nature* **436**, 261–265 (2005).
47. J. T. Trachtenberg *et al.*, "Long-term *in vivo* imaging of experience-dependent synaptic plasticity in adult cortex," *Nature* **420**, 788–794 (2002).

48. V. De Paola *et al.*, "Cell type-specific structural plasticity of axonal branches and boutons in the adult neocortex," *Neuron* **49**, 861–875 (2006).
49. D. D. Stettler, H. Yamahachi, W. Li, W. Denk, C. D. Gilbert, "Axons and synaptic boutons are highly dynamic in adult visual cortex," *Neuron* **49**, 877–887 (2006).
50. L. V. Wang, "Multiscale photoacoustic microscopy and computed tomography," *Nat. Photonics* **3**, 503–509 (2009).
51. X. Q. Yang, X. Cai, K. Maslov, L. H. Wang, Q. M. Luo, "High-resolution photoacoustic microscope for rat brain imaging *in vivo*," *Chin. Opt. Lett.* **8**, 609–611 (2010).
52. F. Helmchen, W. Denk, "Deep tissue two-photon microscopy," *Nat. Methods* **2**, 932–940 (2005).
53. K. Svoboda, R. Yasuda, "Principles of two-photon excitation microscopy and its applications to neuroscience," *Neuron* **50**, 823–839 (2006).
54. A. Holtmaat *et al.*, "Long-term, high-resolution imaging in the mouse neocortex through a chronic cranial window," *Nat. Protoc.* **4**, 1128–1144 (2009).
55. L. Aigner *et al.*, "Overexpression of the neural growth-associated protein GAP-43 induces nerve sprouting in the adult nervous system of transgenic mice," *Cell* **83**, 269–278 (1995).
56. C. Beaulieu, M. Colonnier, "Effect of the richness of the environment on the cat visual cortex," *J. Comp. Neurol.* **266**, 478–494 (1987).
57. W. T. Greenough, H. M. Hwang, C. Gorman, "Evidence for active synapse formation or altered postsynaptic metabolism in visual cortex of rats reared in complex environments," *Proc. Natl. Acad. Sci. USA* **82**, 4549–4552 (1985).
58. B. Kolb, J. Cioe, W. Comeau, "Contrasting effects of motor and visual spatial learning tasks on dendritic arborization and spine density in rats," *Neurobiol. Learn. Mem.* **90**, 295–300 (2008).
59. M. B. Moser, "Making more synapses: A way to store information?," *Cell. Molec. Life Sci.* **55**, 593–600 (1999).
60. M. B. Moser, M. Trommald, P. Andersen, "An increase in dendritic spine density on hippocampal CA1 pyramidal cells following spatial learning in adult rats suggests the formation of new synapses," *Proc. Natl. Acad. Sci. USA* **91**, 12,673–12,675 (1994).
61. G. W. Knott, C. Quairiaux, C. Genoud, E. Welker, "Formation of dendritic spines with GABAergic synapses induced by whisker stimulation in adult mice," *Neuron* **34**, 265–273 (2002).
62. C. E. Brown, P. Li, J. D. Boyd, K. R. Delaney, T. H. Murphy, "Extensive turnover of dendritic spines and vascular remodeling in cortical tissues recovering from stroke," *J. Neurosci.* **27**, 4101–4109 (2007).
63. N. Dancause *et al.*, "Extensive cortical rewiring after brain injury," *J. Neurosci.* **25**, 10,167–10,179 (2005).
64. T. Schallert, J. L. Leasure, B. Kolb, "Experience-associated structural events, subependymal cellular proliferative activity, and functional recovery after injury to the central nervous system," *J. Cereb. Blood Flow Metab.* **20**, 1513–1528 (2000).
65. P. Strata, A. Buffo, F. Rossi, "Regenerative events in the olivocerebellar pathway," *Restor. Neurol. Neurosci.* **19**, 95–106 (2001).
66. A. Buffo, M. Fronte, A. B. Oestreicher, F. Rossi, "Degenerative phenomena and reactive modifications of the adult rat inferior olivary neurons following axotomy and disconnection from their targets," *Neuroscience* **85**, 587–604 (1998).
67. K. König, I. Riemann, P. Fischer, K. J. Halhuber, "Intracellular nanosurgery with near infrared femtosecond laser pulses," *Cell. Molec. Biol. (Noisy-le-grand)* **45**, 195–201 (1999).
68. S. Kumar *et al.*, "Viscoelastic retraction of single living stress fibers and its impact on cell shape, cytoskeletal organization, and extracellular matrix mechanics," *Biophys. J.* **90**, 3762–3773 (2006).
69. L. Sacconi, I. M. Tolic-Norrelykke, R. Antolini, F. S. Pavone, "Combined intracellular three-dimensional imaging and selective nanosurgery by a nonlinear microscope," *J. Biomed. Opt.* **10**, 14002 (2005).
70. N. Shen *et al.*, "Ablation of cytoskeletal filaments and mitochondria in live cells using a femtosecond laser nanoscissor," *Mech. Chem. Biosyst.* **2**, 17–25 (2005).
71. I. M. Tolic-Norrelykke, L. Sacconi, G. Thon, F. S. Pavone, "Positioning and elongation of the fission yeast spindle by microtubule-based pushing," *Curr. Biol.* **14**, 1181–1186 (2004).
72. V. Kohli, A. Y. Elezzabi, "Laser surgery of zebrafish (*Danio rerio*) embryos using femtosecond laser pulses: Optimal parameters for exogenous material delivery, and the laser's effect on short- and long-term development," *BMC Biotechnol.* **8**, 7 (2008).
73. L. Sacconi *et al.*, "In vivo multiphoton nanosurgery on cortical neurons," *J. Biomed. Opt.* **12**, 050502 (2007).
74. A. L. Allegra Mascaro, L. Sacconi, F. S. Pavone, "Multi-photon nanosurgery in live brain," *Front Neuroenergetics* **2**, 21 (2010).
75. P. S. Tsai *et al.*, "Plasma-mediated ablation: An optical tool for submicrometer surgery on neuronal and vascular systems," *Curr. Opin. Biotechnol.* **20**, 90–99 (2009).

76. N. Nishimura *et al.*, "Targeted insult to subsurface cortical blood vessels using ultrashort laser pulses: Three models of stroke," *Nat. Methods* **3**, 99–108 (2006).
77. R. Yasuda *et al.*, "Imaging calcium concentration dynamics in small neuronal compartments," *Sci. STKE* **2004**, p. 15 (2004).
78. E. A. Nimchinsky, R. Yasuda, T. G. Oertner, K. Svoboda, "The number of glutamate receptors opened by synaptic stimulation in single hippocampal spines," *J. Neurosci.* **24**, 2054–2064 (2004).
79. B. L. Sabatini, K. Svoboda, "Analysis of calcium channels in single spines using optical fluctuation analysis," *Nature* **408**, 589–593 (2000).
80. R. Yasuda, B. L. Sabatini, K. Svoboda, "Plasticity of calcium channels in dendritic spines," *Nat. Neurosci.* **6**, 948–955 (2003).
81. V. Egger, K. Svoboda, Z. F. Mainen, "Dendrodendritic synaptic signals in olfactory bulb granule cells: Local spine boost and global low-threshold spike," *J. Neurosci.* **25**, 3521–3530 (2005).
82. J. H. Goldberg, C. O. Lacefield, R. Yuste, "Global dendritic calcium spikes in mouse layer 5 low threshold spiking interneurons: Implications for control of pyramidal cell bursting," *J. Physiol.* **558**, 465–478 (2004).
83. T. Nevian, B. Sakmann, "Single spine Ca^{2+} signals evoked by coincident EPSPs and backpropagating action potentials in spiny stellate cells of layer 4 in the juvenile rat somatosensory barrel cortex," *J. Neurosci.* **24**, 1689–1699 (2004).
84. B. Rozsa, T. Zelles, E. S. Vizi, B. Lendvai, "Distance-dependent scaling of calcium transients evoked by backpropagating spikes and synaptic activity in dendrites of hippocampal interneurons," *J. Neurosci.* **24**, 661–670 (2004).
85. C. L. Cox, W. Denk, D. W. Tank, K. Svoboda, "Action potentials reliably invade axonal arbors of rat neocortical neurons," *Proc. Natl. Acad. Sci. USA* **97**, 9724–9728 (2000).
86. H. J. Koester, B. Sakmann, "Calcium dynamics associated with action potentials in single nerve terminals of pyramidal cells in layer 2/3 of the young rat neocortex," *J. Physiol.* **529 Pt 3**, 625–646 (2000).
87. D. A. Rusakov, A. Wuerz, D. M. Kullmann, "Heterogeneity and specificity of presynaptic Ca^{2+} current modulation by mGluRs at individual hippocampal synapses," *Cereb. Cortex* **14**, 748–758 (2004).
88. R. Cossart, Y. Ikegaya, R. Yuste, "Calcium imaging of cortical networks dynamics," *Cell Calcium* **37**, 451–457 (2005).
89. F. Helmchen, K. Imoto, B. Sakmann, " Ca^{2+} buffering and action potential-evoked Ca^{2+} signaling in dendrites of pyramidal neurons," *Biophys. J.* **70**, 1069–1081 (1996).
90. M. Maravall, Z. F. Mainen, B. L. Sabatini, K. Svoboda, "Estimating intracellular calcium concentrations and buffering without wavelength ratioing," *Biophys. J.* **78**, 2655–2667 (2000).
91. K. Svoboda, W. Denk, D. Kleinfeld, D. W. Tank, "*In vivo* dendritic calcium dynamics in neocortical pyramidal neurons," *Nature* **385**, 161–165 (1997).
92. E. Neher, B. Sakmann, "Single-channel currents recorded from membrane of denervated frog muscle fibres," *Nature* **260**, 799–802 (1976).
93. J. Mapelli, E. D'Angelo, "The spatial organization of long-term synaptic plasticity at the input stage of cerebellum," *J. Neurosci.* **27**, 1285–1296 (2007).
94. U. Egert, D. Heck, A. Aertsen, "Two-dimensional monitoring of spiking networks in acute brain slices," *Exp. Brain. Res.* **142**, 268–274 (2002).
95. L. B. Cohen, B. M. Salzberg, "Optical measurement of membrane potential," *Rev. Physiol. Biochem. Pharmacol.* **83**, 35–88 (1978).
96. D. S. Peterka, H. Takahashi, R. Yuste, "Imaging voltage in neurons," *Neuron* **69**, 9–21 (2011).
97. L. Moreaux, O. Sandre, S. Charpak, M. Blanchard-Desce, J. Mertz, "Coherent scattering in multi-harmonic light microscopy," *Biophys. J.* **80**, 1568–1574 (2001).
98. P. J. Campagnola, L. M. Loew, "Second-harmonic imaging microscopy for visualizing biomolecular arrays in cells, tissues and organisms," *Nat. Biotechnol.* **21**, 1356–1360 (2003).
99. L. Sacconi *et al.*, "Cell imaging and manipulation by nonlinear optical microscopy," *Cell Biochem. Biophys.* **45**, 289–302 (2006).
100. F. Vanzi, L. Sacconi, R. Cicchi, F. S. Pavone, "Protein conformation and molecular order probed by second-harmonic-generation microscopy," *J. Biomed. Opt.* **17**, 060901 (2012).
101. T. Pons, L. Moreaux, O. Mongin, M. Blanchard-Desce, J. Mertz, "Mechanisms of membrane potential sensing with second-harmonic generation microscopy," *J. Biomed. Opt.* **8**, 428–431 (2003).
102. D. A. Dombeck, M. Blanchard-Desce, W. W. Webb, "Optical recording of action potentials with second-harmonic generation microscopy," *J. Neurosci.* **24**, 999–1003 (2004).
103. L. Sacconi, D. A. Dombeck, W. W. Webb, "Overcoming photodamage in second-harmonic generation microscopy: Real-time optical recording of neuronal action potentials," *Proc. Natl. Acad. Sci. USA* **103**, 3124–3129 (2006).
104. D. A. Dombeck, L. Sacconi, M. Blanchard-Desce, W. W. Webb, "Optical recording of fast neuronal membrane potential transients in acute mammalian brain slices by second-harmonic generation

- microscopy,” *J. Neurophysiol.* **94**, 3628–3636 (2005).
105. M. Nuriya, J. Jiang, B. Nemet, K. B. Eisenthal, R. Yuste, “Imaging membrane potential in dendritic spines,” *Proc. Natl. Acad. Sci. USA* **103**, 786–790 (2006).
106. A. Bullen, S. S. Patel, P. Saggau, “High-speed, random-access fluorescence microscopy: I. High-resolution optical recording with voltage-sensitive dyes and ion indicators,” *Biophys. J.* **73**, 477–491 (1997).
107. L. Sacconi *et al.*, “Optical recording of electrical activity in intact neuronal networks with random access second-harmonic generation microscopy,” *Opt. Express* **16**, 14910–14921 (2008).
108. J. A. Fisher *et al.*, “Two-photon excitation of potentiometric probes enables optical recording of action potentials from mammalian nerve terminals *in situ*,” *J. Neurophysiol.* **99**, 1545–1553 (2008).
109. L. Sacconi *et al.*, “Action potential propagation in transverse-axial tubular system is impaired in heart failure,” *Proc. Natl. Acad. Sci. USA* **109**, 5815–5819 (2012).
110. S. Shoham, D. H. O’Connor, R. Segev, “How silent is the brain: Is there a ‘dark matter’ problem in neuroscience?,” *J. Comp. Physiol. A Neuroethol. Sens. Neural. Behav. Physiol.* **192**, 777–784 (2006).
111. V. Nikolenko, K. E. Poskanzer, R. Yuste, “Two-photon photostimulation and imaging of neural circuits,” *Nat. Methods* **4**, 943–950 (2007).
112. A. Holtmaat and K. Svoboda, “Experience-dependent structural synaptic plasticity in the mammalian brain,” *Nat. Rev. Neurosci.* **10**, 647–658 (2009).